MULTI-OBJECTIVE OPTIMIZATION OF THREE ROWS OF FILM COOLING HOLES BY GENETIC ALGORITHM

by

Yaser TAHERI[a], Meran Rajabi ZARGARABADI[a*], and Mehdi JAHROMI[b]

[a] Faculty of Mechanical Engineering, Semnan University, Semnan, Iran
[b] Malek Ashtar University of Technology, Tehran, Iran

Original scientific paper
https://doi.org/10.2298/TSCI190805230T

Aero-thermal optimization on multi-rows of film cooling over a flat plate has been performed to optimize the inclination angles. Hence three cylindrical holes with injection angles of α, β, and γ have been considered. The cooling hole has a 3 mm diameter and an inclined angle between 25-35°. Numerical simulations were performed at a fixed density ratio of 1.25 and blowing ratio of 0.5. The control-volume method with a SIMPLEC algorithm has been used to solve the steady-state RANS equations with SST k-ω turbulent model. The injection angles of the holes are selected as the design variables to perform the optimization of three rows of film cooling. In order to evaluate the performance of holes arrangement, two objective functions are defined based on aerodynamic losses and adiabatic film cooling effectiveness. The curve fitting method is used to find the optimal point of objective functions. The optimizations have been performed using the genetic algorithm method. Results of the present study show that the best performance of three rows of cooling holes was achieved in inclined angles 25.45, 32.85, and 33.1.

Key words: *film cooling, genetic algorithm, inclined angle, numerical simulation*

Introduction

In the modern gas turbines, substantial effort for increasing the thermal efficiency is directed to increase the inlet temperature of the turbine. Internal convection cooling and external film cooling should be applied to keep desirable life and operational demands under high temperature gases [1, 2]. The film cooling performance is highly affected by the hole shape and operating conditions [3-6].

Over the past decades, the numerical and experimental studies have been accomplished to understand the fundamental physics of film cooling flows [7]. Andrew *et al.* [8] studied normal (90º) and inclined holes (30º and 150º) and show that the inclined holes give better performance in comparison with normal holes. Abdullah and Funazaki [9] studied four rows of different inclined holes with two different angles of 20° and 35° and showed that more cooling effectiveness was achieved at a shallow hole angle of $\alpha = 20°$.

Sarkar and Bose [10] showed that increasing the injection angle resulting in increasing the penetration of cooling air into the cross-flow which led to higher turbulence generation and reduction of cooling performance. Furthermore, the effects of cylindrical holes injection angle on the performance of cooling were simulated by Nasir *et al.* [11], Shine *et al.* [12], and

* Corresponding author, e-mail: rajabi@semnan.ac.ir

Hale *et al.* [13]. They highlighted that lower stream-wise injection angles perform better by producing a higher film cooling effectiveness. Yuen *et al.* [14] considered the effectiveness of film cooling by rows of cylindrical holes with different injection angles. Their experimental results show that the maximum efficiency corresponds to the injection angle of 30º. Guangchao *et al.* [15] investigated the effect of injection angle on cooling performance of dual fanned holes.

Yuzhen *et al.* [16] results showed that the row spacing ratio affects the film cooling performance. They found that, better adiabatic cooling performance is achieved by using a smaller pitch, especially for the multi-hole patterns. Ai and Fletcher [17] concluded that for small hole spacing the cooling effectiveness at the area near to the exit of coolant is slightly higher than large hole spacing. Cun-Liang *et al.* [18] concluded that interaction between the adjacent jets at the hole spacing with small values lead to better effectiveness than large hole spacing at downstream locations.

Film cooling is a complex technique and a large number of geometrical parameters and flow can effect on this technique. Researchers have to considered multi-dimensional design space to find a global optimum solution. Lee and Kim [19] used coupling Kriging model and sequential quadratic programming to optimize a shaped hole. Johnson *et al.* [20] applied the genetic algorithm (GA) to optimize the film cooling array of a high pressure turbine on the vane pressure side. A multi-objective technique is performed by Lee *et al*. [21] to optimize a shape of one row of fan shape holes. Ayoubi *et al*. [22] optimized a round shape cooling hole by developing a non-dominated sorting GA. They improved the film cooling effectiveness over the surface while reducing the aerodynamic losses. Wang *et al*. [23] optimized of a fan-shaped hole by coupling the RBF neural network and GA. In general, previous studies are focused only to optimize the averaged film cooling effectiveness through the hole shape [21-24].

The aim of the present numerical study is to investigate the effects of the inclined angles of three rows of cylindrical holes on area-averaged film cooling effectiveness and pressure difference, simultaneously. Optimum point of inclined angles is found with optimization of the objective functions by using the GA. A set of optimal designs were presented as Pareto-optimal solutions.

Computational domain

The computational domain of the present study has been shown in fig. 1. Injection angle of each cylindrical hole with 3 mm diameters is varied from 25°-35°. It is essential to model plenum, film hole and the cross-flow regions simultaneously for a detailed demonstration of interaction between jet and cross-flow [25]. The plenum is as a supplier of the cooling air and coolant enters the cross-flow area through the film hole. The computational model was extend-

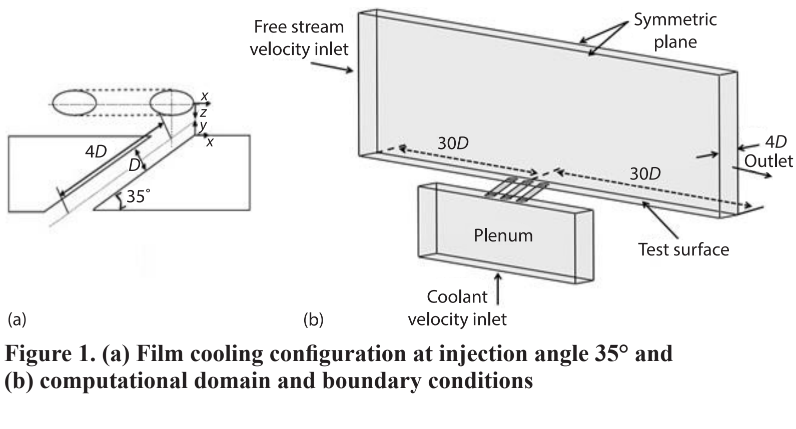

Figure 1. (a) Film cooling configuration at injection angle 35° and (b) computational domain and boundary conditions

ed 50 mm high from the test surface. The uniform air velocity is set for plenum inlet to apply the desired blowing ratio ($M = 0.5$). The operating parameters used to compute the performance of the film cooling process was given in tab. 1.

Turbulence intensity is assumed to be 0.2% and 0.1% for free stream and coolant, respectively. Two lateral planes in the mainstream duct were assumed symmetry boundary condition. The top surface of mainstream duct is away from the test plate sufficiently and this is a reason that top surface defined as symmetry plane. Velocity inlet boundary condition was defined for the freestream and coolant inlet, and outflow boundary condition was applied at the outlet surface of mainstream duct, whereas the plate, coolant-pipe, and plenum were modeled as an adiabatic wall with the no-slip condition. The spacing of two rows of coolant holes in the streamwise direction is 5D and the spacing between center-to-center of adjacent holes was set to 4D.

Table 1. operating parameters

Property	Value
Freestream temperature	373.15 K
Blowing ratio	0.5
Density ratio	1.25
Coolant temperature	298.15 K

Numerical method

In the present study, the governing equations have been solved using ANSYS FLUENT 16.0.0 [26] to find the effects of the design variables on the objective functions. The steady-state Reynolds averaged Navier-Stokes equations, can be written:

$$\frac{\partial U_i}{\partial x_i} = 0 \tag{1}$$

$$\rho U_i \frac{\partial U_i}{\partial x_i} = -\frac{\partial p}{\partial x_j} + \mu \frac{\partial^2 \Theta}{\partial x_i \partial x_i} - \frac{\partial}{\partial x_i}\left(\rho \overline{u_i u_j}\right) \tag{2}$$

$$U_i \frac{\partial \Theta}{\partial x_i} = \alpha \frac{\partial^2 \Theta}{\partial x_i \partial x_i} - \frac{\partial}{\partial x_i}\left(\overline{u_i \theta}\right) \tag{3}$$

where $\overline{u_i u_j}$ and $\overline{u_i \theta}$ are known as the Reynolds stress tensor and the turbulent heat flux vector, respectively. The SST k-ω turbulence model is more accurate and reliable for a wide class of flows (*e.g.*, adverse pressure gradient flows, air-foils and jet in cross-flow) in comparison with the standard k-ω and the standard k-ε models. Details of the mathematical formulation can be found in [26, 27]. The pressure-velocity coupling was performed by the SIMPLEC algorithm.

Structural meshes, fig. 2, were constructed by using ANSYS ICEM and grid nodes near the wall refined significantly where the first layer grid height is set to be small enough to make sure that Y PLUS value at the near-wall cell should be of the order of 1. The grid sensitivity test for lower bound is given in fig. 3. Three grids with different density and numbers of cells have been generated to achieve the optimal number of cells. Therefore, the grid with 1057095 cells has been selected for the computations. The adiabatic film cooling effectiveness on the centerline can be predicted directly by using:

$$\eta = \frac{T_{\text{aw}} - T_\infty}{T_c - T_\infty} \tag{4}$$

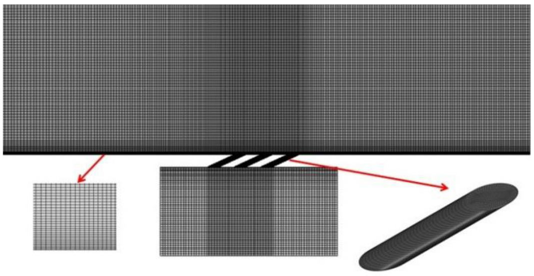

Figure 2. An example of the computational grid

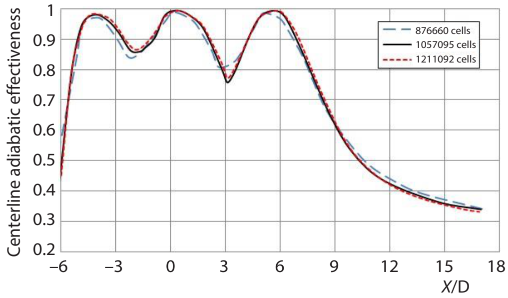

Figure 3. Grid sensitivity test

Objective functions and design variables

In the present study, aero-thermal optimization on multi-rows film cooling holes has been performed. Hence two objective functions based on adiabatic cooling effectiveness and aerodynamic losses have been defined. The non-dimensional pressure ($\Delta P/P_{\text{plenum}}$), is chosen as the objective functions for aerodynamic loss. The averaged film-cooling effectiveness over the test surface has been considered as the objective function for film cooling performance:

$$\overline{\eta}\left(x,z\right)=\frac{1}{4D\times 23D}\int_{-2D}^{2D}\int_{-5D}^{17D}\eta\left(x,z\right)\mathrm{d}x\mathrm{d}z \tag{5}$$

In the present study, three geometrical parameters have been considered as design variables. These parameters including the injection angle of the holes α, β, and γ. These angles are shown in fig. 4. The results of previous numerical studies have been considered in selecting the ranges of the design variables. Also, primary simulations for each design variable have been accomplished in wide ranges. These design variables and ultimate ranges are given in tab. 2.

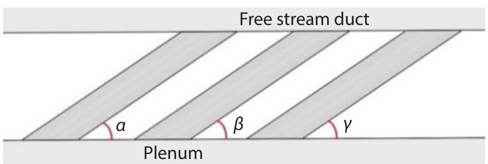

Figure 4. Schematic view of three design variables

Table 2. Lower and upper limits of the design variables

Design variables	Lower bound	Upper bound
α [°]	25	35
β [°]	25	35
γ [°]	25	35

Optimization procedure

The optimization procedure has been used in this study is shown in fig. 5. Three design variables are chosen, and the design space was determined at first. At the design points, Numerical simulation is used to compute the values of objective function. Multi-objective optimization needs many assessments of the objective function find the optimal solutions. In the present study, the objective function values are evaluated by the curve fitting method (CFM), which prevents numerical cost. The CFM is based on a methodology that fits the sum of exponential or polynomial functions to numerical simulation results.

Results and discussion

Twenty seven cooling holes configurations are modeled to considered the effect of design variables on the objective function. From these 27 configurations, 20 groups have been selected for initial population or training samples (TRS). The remaining (7 groups) are also considered for the testing sample (TES). Numerical simulations have been done for all 27 cooling configurations. In the present study, initial population is chosen accidentally from all configurations, and the randomly design points are spread through the design space evenly.

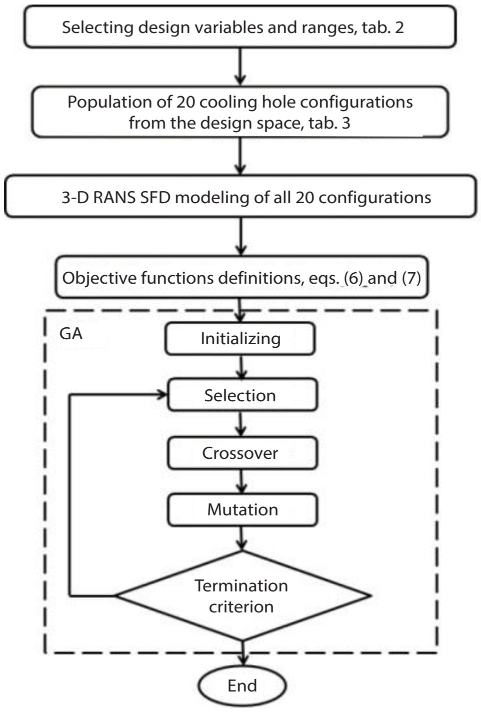

Figure 5. Optimization procedure

Figure 6 shows the non-dimensional temperature contours at x/d = 0, 5, and 9 for upper (three holes with inclined angles 35°) and lower bound (three holes with inclined angles 25°) of the configurations. The jets interaction with cross-flow is more when large streamwise angle are used and consequently due to jet lift-off, the mainstream penetrates more into the jets flow [11]. In the downstream, the coolant air is moved away from the wall due to the presence of the counter-rotating vortex structure. These vortex structures push the cooling air upward and pull the hot mainstream gases toward the wall. As expected, move away from the coolant jet/wake from the wall along the centerline is higher for upper bound rather than lower bound configuration.

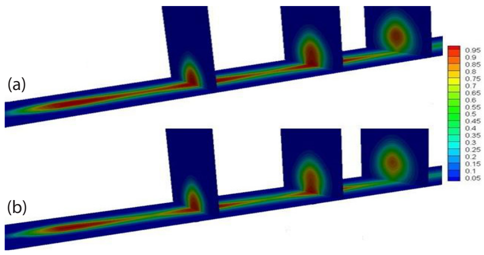

Figure 6. Contours of non-dimensional temperature at x/d = 0, 5, 9 for (a) lower and (b) upper bound

Figure 7 shows a pair of symmetric vortices (kidney vortices), which are created due to the interaction between the cooling air and hot mainstream. These kidney vortices significantly

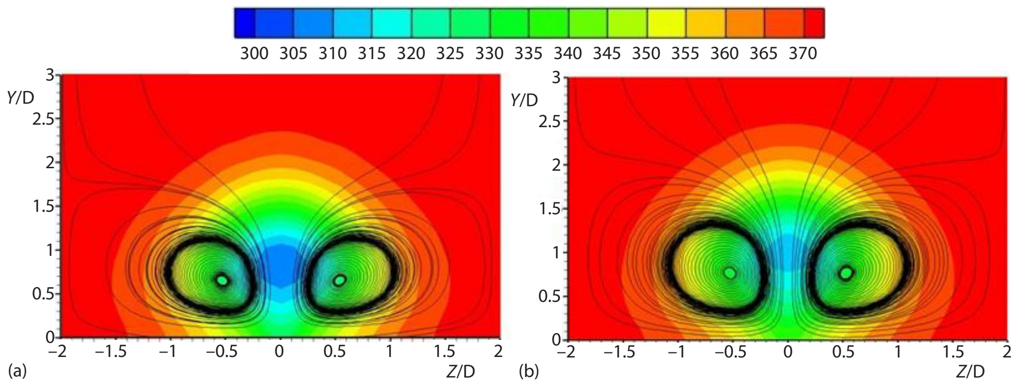

Figure 7. Vortex structure at x/d = 9 for (a) lower and (b) upper bound, temperature contour in [K]

reduce the effectiveness of film cooling by pushing the coolant from the target surface. This figure also shows that center of the counter-rotating vortexes for the lower band is closer to the surface than those obtained for the upper band. This is the main reason for higher film cooling effectiveness in this case. As shown in fig. 6(a), the holes with three inclined angles 25°, show better adiabatic effectiveness on the test surface. The objective functions values for each design variable in the initial population are listed in tab. 3.

The adiabatic effectiveness results from the simulations showed significant improvements from the lower bound when compared to upper bound configuration. This table shows that reducing the inclined angles from 35-25°, will result in approximately 21% increasing in area-averaged film cooling effectiveness, as mentioned by previous studies [11-14]. But it is notable that, reducing the inclined angles will also leads to increasing in pressure difference. The difference between the averages of the three jets output pressure and the inlet pressure of the plenum is increased from 27.711-34.034 Pa, that's means approximately 23% increasing in pressure difference.

Table 3. Values of design variables and objective functions

Initial configurations	Design variables			Objective functions	
	α [°]	β [°]	γ [°]	$\bar{\eta}$	$\Delta P/P_{\text{plenum}}$
TRS 1	25	25	25	0.339	0.6219
TRS 2	25	25	30	0.333	0.6081
TRS 3	25	30	25	0.3308	0.6068
TRS 4	25	30	35	0.3213	0.5784
TRS 5	25	35	30	0.3178	0.5838
TRS 6	25	35	35	0.3126	0.5692
TRS 7	30	25	25	0.3171	0.6141
TRS 8	30	25	35	0.3075	0.5851
TRS 9	30	30	25	0.3096	0.5985
TRS 10	30	30	30	0.3049	0.5812
TRS 11	30	30	35	0.301	0.567
TRS 12	30	35	30	0.2966	0.5732
TRS 13	30	35	35	0.2928	0.5576
TRS 14	35	25	30	0.2958	0.5922
TRS 15	35	25	35	0.2936	0.579
TRS 16	35	30	25	0.2959	0.5922
TRS 17	35	30	30	0.2903	0.5737
TRS 18	35	35	25	0.2885	0.5829
TRS 19	35	35	30	0.2834	0.5634
TRS 20	35	35	35	0.2801	0.5474

The relationship between the objective functions and design variables are obtained by using curve fitting. This method (CFM) is usually applied for analyzing the results of numerical and experimental studies in film cooling technique [28-31]. The optimum design point can be detected by the following curve fittings equations:

$$\overline{\eta} = 0.2354\left(\tan\alpha\right)^{-0.2812}\left(\tan\beta\right)^{-0.116}\left(\tan\gamma\right)^{-0.07792} \tag{6}$$

$$\frac{\Delta P}{P_{\text{plenum}}} = 0.494\left(\tan\alpha\right)^{-0.0701}\left(\tan\beta\right)^{-0.1106}\left(\tan\gamma\right)^{-0.124} \tag{7}$$

Seven TES were used to evaluate the accuracy of CFM method *vs.* the numerical simulation. These TES are listed in tab. 4. With these curve fittings, the maximum error in predicting the objective functions are approximately 1.5% and 0.8% for area-averaged film cooling effectiveness, η, and aerodynamic loss, respectively.

Table 4. Testing samples

Testing sample	Design variables			Objective function 1 ($\overline{\eta}$)		Objective function 2 ($\Delta P/P_{\text{plenum}}$)	
	α [°]	β [°]	γ [°]	Predicted by CFM	Predicted by CFD	Predicted by CFM	Predicted by CFD
TES 1	25	25	35	0.3278	0.323	0.5928	0.596
TES 2	25	30	30	0.3246	0.3253	0.5929	0.5924
TES 3	25	35	25	0.3228	0.3215	0.596	0.6006
TES 4	30	25	30	0.3134	0.3114	0.5981	0.5979
TES 5	30	35	25	0.3039	0.3015	0.5871	0.5909
TES 6	35	25	25	0.3018	0.3019	0.6059	0.6074
TES 7	35	30	35	0.2852	0.2868	0.5627	0.5581

In the present study, the cooling optimization has been done based on the GA. For film cooling applications, satisfactory solutions can be given quickly by GA [20, 24]. Darwin's theory of evolution is the motivation of the GA. Finding the best available global design is the purpose of the GA process. In this study, the GA is written in C programming language.

The present study aims are to find an optimum point which in this point, the area-averaged film cooling effectiveness has a maximum value and the ratio of the pressure difference to the inlet pressure of the plenum is also minimized. A set of optimal designs have been presented as Pareto-optimal solutions. With this process, the optimum point of design variables α, β, and γ are 25.45, 32.85, and 33.1, respectively.

Numerical simulation has also been used for the optimal point which concluded from CFM-GA (α = 25.45°, β = 32.85°, and γ = 33.1°). The film cooling effectiveness and the ratio of the pressure difference to the inlet pressure of the plenum at optimal points are compared in tab. 5. The optimal film cooling effectiveness gained from CFM and CFD simulation are 0.315 and 0.316, respectively. Also, the optimal ratio of the pressure difference to the inlet pressure of the plenum calculated from CFM and RANS solution is 0.576 and 0.577, respectively, and the difference between these values is less than 0.2%.

Table 5. Comparison of objective functions predicted by CFM and CFD at the optimal point

	Design variables			Objective function 1 ($\overline{\eta}$)		Objective function 2 ($\Delta P/P_{\text{plenum}}$)	
	α [°]	β [°]	γ [°]	Predicted by CFM	Predicted by CFD	Predicted by CFM	Predicted by CFD
Optimal design by GA	25.45	32.85	33.1	0.315	0.316	0.576	0.577

Figure 8 compares the centerline adiabatic effectiveness at $M = 0.5$. As mentioned by Walters and Leylek [32] the pressure gradient in the injection region causes the increase of the momentum of the fluid in the downstream region of the jet exit. At the streamwise inclination of 35°, the effectiveness is lower than that for 25° streamwise injections, as the higher streamwise angle lead to greater jet penetration and result in lower coolant coverage. Under a specified blowing ratio ($M = 0.5$), the three holes with inclined angles 35° shows a lower film cooling effectiveness in comparison with other cases. When the multi-hole injection with inclined angles 25° is used, the decrease in strength of kidney vortices leads to a significant increase of the film cooling effectiveness. The most notable improvement of the film cooling effectiveness is considered in the between of the holes region. The optimum design that is calculated by the GA improves the distributions of the film-cooling effectiveness along the centerline in comparison with the upper bound case.

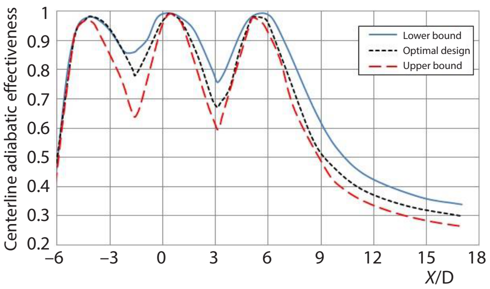

Figure 8. Centerline film cooling effectiveness for lower, optimum, and upper bound angles

Figure 9 shows the film-cooling effectiveness contours on the test surface for optimum and original geometries (upper and lower bound cases) at different x/d. According to these figures and previous studies [11-14], the distribution of cooling air for the three holes with inclined angles 35° is lower than other cases in both directions (streamwise and spanwise). This can be the consequence of the jet lift-off and the dilution of the coolant air downstream of the film hole, as shown in fig. 6, which results in low cooling effectiveness. These figures also show that the penetration of the holes with inclined angles 25° is weaker than that for the other cases. As shown in fig. 9, the inclined angles of multi-hole arrangement, can significantly affect the distribution of the adiabatic film cooling effectiveness.

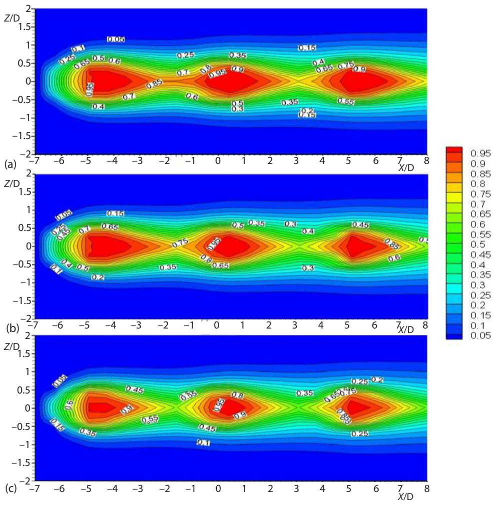

Figure 9. Contours of film cooling effectiveness on the test surface at $-7 < x/d < 8$ for (a) lower bound condition, (b) optimum design, and (c) upper bound condition

The comparison of the two objective functions at optimal design point and reference geometries is shown in fig. 10. This chart shows that the optimized shape improved area-averaged film-cooling effectiveness over the test surface by approximately 13% in comparison with the upper bound reference geometry. Also, this shape improved second objective function ($\Delta P/P_{plenum}$) by approximately 8% in comparison with the lower bound reference geometry.

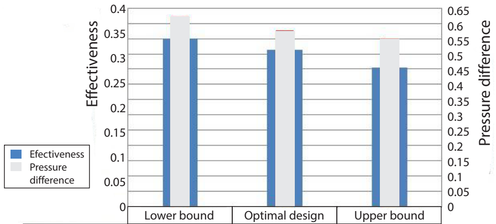

	Lower bound	Optimal design	Upper bound
Effectiveness	0.339	0.316	0.2801
Pressure difference	0.6219	0.577	0.5474

Figure 10. Comparison of objective functions predicted by CFD

Effect of the different blowing ratio on the second objective function ($\Delta P/P_{\text{plenum}}$) is shown in fig. 11. Eight blowing ratios, included M = 0.3, 0.5, 0.8, 1, 1.5, 2, 2.5, and 3, were investigated for this plot. Since the optimum and reference geometries show a similar trend, therefore, the optimum and lower geometries are selected for display. The pressure ratio was inversely proportional to the area-averaged film cooling effectiveness. The high momentum of the cooling air forms a strong CRVP with increasing of blowing ratio, which lifts the cooling air from the target surface and consequently the cooling air replaces with the hot mainstream in the near-wall region [4]. This results in decreasing film cooling effectiveness [11]. As shown in fig. 11, the pressure ratio increase with increasing the blowing ratios. For M < 1.0, the increasing trend of the second objective function is more significant, especially between the blowing ratios 0.3-0.8.

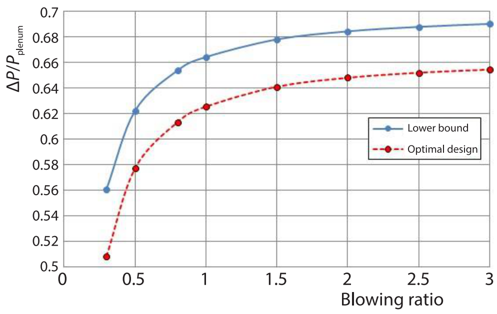

Figure 11. Effect of the blowing ratio on the pressure ratio

Conclusions

The optimization of film cooling performance was carried out numerically by GA. The numerical investigation is performed on three rows of the cylindrical holes which every hole has a 3 mm diameter and the inclined angle between 25-35°. Numerical simulations are done at a fixed density ratio and blowing of 1.25 and 0.5, respectively. The spacing of two rows of coolant holes in the streamwise direction is 5D and the spacing between center-to-center of adjacent holes was set to 4D. The control-volume method with a SIMPLEC algorithm has been used to solve the steady-state RANS equations. The turbulent flow and heat transfer are modeled with the k-ω SST turbulence model. Reducing the inclined angles from 35-25° will result in approximately 21% increase in area-averaged film cooling effectiveness. It is notable that, reducing the inclined angles results in an increase in the pressure difference between the averages of the jets output pressure and inlet pressure of the plenum.

For the three design variables, namely, the inclined angles, 20 groups of TRS and seven groups of TES are generated. Optimizations have been performed for two objective functions, which are defined as area-averaged film cooling effectiveness, $\overline{\eta}$, and the ratio of the pressure difference to the inlet pressure of the plenum ($\Delta P/P_{\text{plenum}}$), simultaneously, and contribution effect of each objective functions on final optimization are the same. As the results, the difference between the value of two objective functions calculated by CFM and CFD was less than 1.5%. The optimum point of the design variables α, β, and γ are found in 25.45°, 32.85°, and 33.1°, respectively. The optimal film cooling effectiveness computed from CFM and RANS solution are 0.315 and 0.316, respectively. The average film cooling effectiveness obtained by CFM has less than 0.4% difference with its value calculated by the numerical simulation. Also, the optimal ratios of the pressure difference to the inlet pressure of the plenum obtained from CFM and CFD are 0.576 and 0.577, respectively, and the difference between these values is less than 0.2%. The optimized shape improved the first objective function by approximately 13% in comparison with the upper bound and the second objective function by approximately 8% in comparison with the lower bound reference geometry.

Nomenclature

D – diameter of the hole, [mm]
k – turbulent kinetic energy, [m^{2}s^{-2}]
M – blowing ratio [$= (\rho U)_c/(\rho U)_\infty$]
T – temperature, [K]
x – x-direction, streamwise distance [mm]
y – y-direction, vertical distance [mm]
z – z-direction, spanwise distance [mm]

Greek symbol

α – injection angle of the 1st hole, [°]
β – injection angle of the 2nd hole, [°]
γ – injection angle of the 3rd hole, [°]
ε – dissipation rate of turbulent kinetic energy, [m^{2}s^{-3}]
η – adiabatic film cooling effectiveness, [$\eta = (T - T_\infty)/(T_C - T_\infty)$]
Θ – internal energy, [J]
θ – heat flux, [Wm^{-2}]
μ – dynamic viscosity, [kgm^{-1}s^{-1}]
ρ – density of the fluid, [kgm^{-3}]

Subscript

aw – adiabatic wall
c – coolant
∞ – free stream

References

[1] Han, J. C., *et al.*, *Gas Turbine Heat Transfer and Cooling Technology*, 2nd ed., Taylor & Francis, New York, USA, 2013
[2] Goldstein, R. J., Film Cooling, *Advances in Heat Transfer*, *7* (1971), pp. 321-379
[3] Zolfagharian, M., *et al.*, Optimization of Turbine Blade Cooling Using Combined Cooling Techniques, *Engineering Applications of Computational Fluid Mechanics*, *8* (2014), 3, pp. 462-475
[4] Xiaokai, S., *et al.*, Influence of Hole Geometry on Film Cooling Effectiveness for a Constant Exit Flow Area, *Applied Thermal Engineering*, *130* (2018), Feb., pp. 1404-1415
[5] Kim, J.-H., Kim, K.-Y., Film-Cooling Performance of Converged-Inlet Hole Shapes, *International Journal of Thermal Sciences*, *124* (2018), Feb., pp. 196-211
[6] Fu, Z., Investigation of the Influence of Inclination Angle and Diffusion Angle on the Film Cooling Performance of Chevron Shaped Hole, J*ournal of Thermal Science*, *27* (2018), 6, pp. 580-591
[7] Huang, K., *et al.*, Experimental Study on Film Cooling Performance of Imperfect Holes, *Chinese Journal of Aeronautics*, *31* (2018), 6, pp. 1215-1221
[8] Andrews, G. E., *et al.*, Full Coverage Effusion Film Cooling with Inclined Holes, *Proceedings*, ASME Inte. Gas Turbine and Aeroengine Cong. and Expo., Houston, Tex., USA, 1995
[9] Abdullah, K., Funazaki, K. I., Effects of Blowing Ratio on Multiple Angle Film Cooling Holes, *Proceedings*, Aerotech IV Conference, Kuala Lumpur, Malaysia, 2012
[10] Sarkar, S., Bose, T. K., Numerical Simulation of a 2-D Jet-Cross-Flow Interaction Related to Film Cooling Applications: Effects of Blowing Rate, Injection Angle and Free-Stream Turbulence, *Sadhana*, *20* (1995), 6, pp. 915- 935
[11] Nasir, H., *et al.*, Effect of Compound Angle Injection on Flat Surface Film Cooling with Large Streamwise Injection Angle, *Experimental Thermal and Fluid Science*, *25* (2001), 1-2, pp. 23-29
[12] Shine, S. R., *et al.*, Internal Wall-Jet Film Cooling with Compound Angle Cylindrical Holes, *Energy Conversion and Management, 68* (2013), Apr., pp. 54-62
[13] Hale, C. A., *et al.*, Film Cooling Effectiveness for Short Film Cooling Holes Fed by a Narrow Plenum, *ASME Journal of Turbomachinery*, *12*2 (2000), 3, pp. 553-557
[14] Yuen, R. F., Martinez-Botas, C. H. N., Film Cooling Characteristics of Rows of Round Holes at Various Streamwise Angles in a Crossflow – Part I: Effectiveness, *International Journal of Heat and Mass Transfer*, *48* (2005), 23-24, pp. 4995-5016
[15] Guangchao, L., *et al*., Film Cooling Performance of a Row of Dual-fanned Holes at Various Injection Angles, *Journal of Thermal Science*, *26* (2017), 5, pp. 453-458
[16] Yuzhen, L., *et al*., Measured Film Cooling Effectiveness of Three Multihole Patterns, *Transactions of ASME*, *128* (2006), 2, pp. 192-197
[17] Ai, W., Fletcher, T. H., Computational Analysis of Conjugate Hea*t Transfer and Particulate Deposition on a High Pressure Turbine Vane,* ASME Journal of Turbomachinery, *134* (2012), 4, pp. 573-585
[18] Cun-liang, L., *et al*., Experimental Investigation on the Leading Edge Film Cooling of Cylindrical and Laid-Back Holes with Different Hole Pitches, *International Journal of Heat and Mass Transfer*, *55* (2012), 23-24, pp. 6832-6845

[19] Lee, K., Kim, K. Y., Surrogate Based Optimization of a Laidback Fan-Shaped Hole for Film-Cooling, *International Journal of Heat Fluid-Flow*, *32* (2011), 1, pp. 226-238
[20] Johnson, J. J., *et al*., Genetic Algorithm Optimization of a High-Pressure Turbine Vane Pressure Side Film Cooling Array, *ASME Journal of Turbomachinery*, *136* (2014), 011011
[21] Lee, K. D., *et al*., Multi-Objective Optimization of a Row of Film Cooling Holes Using an Evolutionary Algorithm and Surrogate Modelling, *Numerical Heat Transfer*, *63* (2013), 8, pp. 623-641
[22] Ayoubi, C. E., *et al*., Aero-Thermal Optimization and Experimental Verification for the Discrete Film Cooling of a Turbine Airfoil, *Proceedings*, ASME Turbo Expo 2013: Turbine Technical Conference and Exposition, San Antonio, Tex., USA, 2013
[23] Wang, C. H., *et al*., Optimization of a Fan Shaped Hole to Improve Film Cooling Performance by RBF Neural Network and Genetic Algorithm, *Aerospace Science and Technology*, *58* (2016), Nov., pp. 18-25
[24] Moeini, A., Zargarabadi, M. R., Genetic Algorithm Optimization of Film Cooling Effectiveness over a Rotating Blade, *International Journal of Thermal Sciences*, *125* (2018), Mar., pp. 248-255
[25] Majumdar, S., *et al*., The 3-D Finite Volume Method for Incompressible Flows with Complex Boundaries, *Journal of Fluids Engineering*, *114* (1992), 4, pp. 496-503
[26] ***, ANSYS Inc. ANSYS FLUENT user's guide, ANSYS FLUENT 16.0.0, Conon-sburg, PA, USA, 2014
[27] Wilcox, D. C., *Turbulence Modelling for CFD*, DCV Industries, Inc., La Canada, Cal., USA, 1993
[28] Yang, X., *et al*., Numerical Simulation of Film Cooling in Hypersonic Flows, *Proceedings*, 36th AIAA Thermophysics Conference, Orlando, Fla., USA, 2003, pp. 23-26
[29] Roy, A., Experimental Study of Gas Turbine Endwall Cooling with Endwall Contouring under Transonic Conditions, Ph. D. thesis, Virginia Polytechnic Institute and State University, Blacksburg, Va., USA, 2014
[30] Xue, S., *et al*., A Novel Transient Technique to Determine Recovery Temperature, Heat Transfer Coefficient, and Film Cooling Effectiveness Simultaneously in a Transonic Turbine Cascade, *Journal of Thermal Science and Engineering Applications*, *7* (2015), 1, 011016-1
[31] Wong, T. H., *et al*., Film Cooling Effectiveness Downstream of Trailing Edge Slots Including Cutback Surface Protuberances, *International Journal of Turbomachinery Propulsion and Power*, *1* (2016), 1, 4
[32] Walters, D. K., Leylek, J. H., A Detailed Analysis of Film-Cooling Physics: Part I – Streamwise Injection with Cylindrical Holes, *ASME Journal of Turbomachinery*, *122* (2000), 1, pp. 102-112

Paper submitted: August 5, 2019
Paper revised: June 1, 2020
Paper accepted: August 22, 2020